D

Dual Nature of Ionic Liquids: Ionic Versus Organic

Rui Shi[1] and Yanting Wang[2,3]
[1]Zhejiang Province Key Laboratory of Quantum Technology and Device, Department of Physics, Zhejiang University, Hangzhou, China
[2]CAS Key Laboratory of Theoretical Physics, Institute of Theoretical Physics, Chinese Academy of Sciences, Beijing, China
[3]China School of Physical Sciences, University of Chinese Academy of Sciences, Beijing, China

Introduction

Inorganic salts consisting solely of inorganic ions usually have high melting temperatures because of the strong Coulomb interactions. Molecular solvents comprised totally of neutral molecules typically show low melting points due to the relatively weak van der Waals (VDW) interactions. Ionic liquids (ILs) consisting of organic ions inherit both ionic and organic nature from inorganic salts and organic liquids.

The dual ionic and organic nature not only brings ILs into liquid phase at room temperature (or below 100 °C) but also provides ILs with many unique properties, which are distinct from both conventional inorganic molten salts and organic solvents. For example, nonflammability, non-volatility, good stability and conductivity that are absent in organic liquids originate from the ionic nature of ILs, whereas good solvability, superior tunability, and low melting temperature that are missing in inorganic molten salts are ascribed to the organic nature of ILs.

Both ionic and organic features strongly depend on the interionic interactions and the underlying liquid structure. Besides charge-charge interactions, in principle, ILs can have all types of interactions characteristic to organic liquids in a tunable manner. For example, the presence and the strength of $\pi - \pi$ [1], H-bond [2, 3], and VDW interactions [4] can be easily tuned by introducing benzene group, hydroxyl group, and alkyl chain to ILs, respectively, which in turn affects the physicochemical properties of ILs. This structural flexibility makes ILs tunable and designable. A better understanding of the dual ionic and organic nature and the underlying interactions is crucial for the theoretical design and practical applications of ILs.

Basic Methodology

Simulation Method

Classical molecular dynamics simulations, accessible to microscopic structures and interactions, are powerful tools to study the structure and interactions of liquids at the atomic level. In a classical force field, the total potential energy is usually separated into bonded and nonbonded interactions. From now on the term "molecule" will be used to refer to both "molecule" and "ion" without

S. Zhang (ed.), *Encyclopedia of Ionic Liquids*,
https://doi.org/10.1007/978-981-10-6739-6_13-1

differentiation. In general, the bonded potential includes intramolecular bond, angle, and dihedral contributions. The nonbonded one V_{nb} between two particles *i, j* is often described by Coulomb and Lennard-Jones potentials by:

$$V_{\mathrm{nb}} = 4\epsilon_{ij}\left[\left(\frac{\sigma_{ij}}{r_{ij}}\right)^{12} - \left(\frac{\sigma_{ij}}{r_{ij}}\right)^{6}\right] + \frac{q_i q_j}{4\pi\epsilon_0 r_{ij}}, \quad (1)$$

where r_{ij} is the distance between two particles *i, j;* q_i is the partial charge of particle *i;* ϵ_0 is the vacuum permittivity; and ϵ_{ij} and σ_{ij} are the VDW parameters. A partial charge is assigned for each particle and a set of VDW parameters are assigned for each pair of particles in the force field. Given the potential function and its parameters, the Newton's equation can thus be easily solved to generate a molecular dynamics trajectory for analysis.

Calculation of Electric Field

In simulation, the average electric field $\boldsymbol{E}$ experienced by a molecule can be directly calculated from the intermolecular Coulomb force by:

$$\boldsymbol{E} = \frac{1}{n}\sum_{i}^{n}\frac{\boldsymbol{F_i}}{q_i}, \quad (2)$$

where n is the number of atoms in the molecule, q_i is the partial charge, and $\boldsymbol{F_i}$ is the Coulomb force experienced by atom *i.*

Calculation of Intermolecular Vibrational Frequency and Force Constant

The vibrational density of state (VDOS) $I(\omega)$ of a system can be calculated from the velocity time correlation function by:

$$I(\omega) = \frac{1}{2\pi k_{\mathrm{B}} T}\sum_{i} m_i \int_{-\infty}^{\infty} \mathrm{d}t \exp\left(-i\omega t\right)\langle v_i(t) v_i(0)\rangle, \quad (3)$$

where k_B is the Boltzmann constant, m_i is the mass of particle *i,* and $v_i(t)$ is the velocity of particle *i* at time *t.* Then the average intermolecular vibrational frequency can be calculated as follows:

$$\langle\omega\rangle = \frac{\int_0^{\omega_c}\omega I(\omega)\mathrm{d}\omega}{\int_0^{\omega_c} I(\omega)\mathrm{d}\omega}. \quad (4)$$

In this calculation, a cutoff frequency ω_c is chosen (typically 500 cm^{-1} for molten NaCl and 175 cm^{-1} for ionic and organic liquids [5]) to exclude all the high frequency intramolecular modes. The mass-scaled vibrational force constant *k,* under the harmonic approximation, can be obtained by:

$$\langle\omega\rangle = \frac{\sqrt{k}}{2\pi c}, \quad (5)$$

where c is the speed of light.

Calculation of Activation Energy

Well above the melting temperature T_m, the temperature dependence of the liquid dynamics, i.e., diffusion coefficient *D,* generally obeys the Arrhenius law,

$$D = D_0 \exp\left(-\frac{E_{\mathrm{a}}}{k_{\mathrm{B}} T}\right), \quad (6)$$

where D_0 is a constant and E_{a} is the activation energy. E_{a} can be obtained by fitting diffusion coefficient data above T_{m} to the Arrhenius law.

Key Findings

Molecular Structure and Charge Delocalization

Seven liquids from three classes were studied [6] by molecular dynamics simulations at the all-atom level: sodium chloride (NaCl) as an archetype of inorganic salts, 1-butyl-3-methylimidazolium nitrate ([BMIm][NO_3]), 1-butyl-3-methylimidazolium tetrafluoroborate ([BMIm][BF_4]), 1-butyl-3-methylimidazolium hexafluorophosphate ([BMIm][PF_6]), 1-butyl-3-methylimidazolium bis(trifluoromethanesulfonyl)imide ([BMIm][NTf_2]) representing typical ILs with different anions, and dimethyl sulfoxide (DMSO) and toluene as widely used polar and weakly polar molecular liquids, respectively. Their molecular structures are shown in Fig. 1.

Molten NaCl, without molecular structure, can be regarded as point charges and thus has a very high charge density. ILs, on the other hand, usually consist of bulky organic ions and thus charges can easily delocalize on each molecule, analogous to organic liquids, which largely reduces the local charge density in ILs. Figure 2a shows the charge distribution in [BMIm][BF_4], compared to that in DMSO and toluene. It can be seen that, despite of the net charge carried by ions, ILs indeed have well-delocalized charge distributions, which is expected to largely soften the Coulomb interactions between ions in ILs.

Liquid Structure and Cage Energy Landscape

Besides charge delocalization, it is shown in the radial distribution function (RDF) in Fig. 2 that ILs have an average ion-ion distance (first peak position) comparable to organic liquids but significantly larger than molten salts. According to the Coulomb's law, the large separation of ions due to the excluded volume of bulky organic ions should further reduces the electrostatic interactions between ions in ILs. This excluded-volume effect, together with charge delocalization, further effectively weakens the Coulomb interactions in ILs, which stems from the organic nature of ILs and is thus absent in inorganic molten salts.

In liquid state, molecules are always surrounded by neighbors which spontaneously form the first coordination shell, resulting in the rise of the first peak in the RDF. The first coordination shell, reacting as a cage in the statistical mechanics manner, encapsulates and traps the central molecule. At the short-time scale, molecules vibrate inside the cage and occasionally escape from the cage and diffuse. The central molecules thus experience an effective cage potential well $U(r)$, whose curvature ($\partial^2 U/\partial r^2$), slope ($-\partial U/\partial r$), and depth ($U_{max} - U_{min}$) generally correspond to the frequency of vibration, the force, and the barrier to escape, respectively. Figure 3 exhibits an example of the cage structure for IL [BMIm][BF_4] and the corresponding schematic of the cage energy landscape.

Intermolecular Vibrational Frequency

Intermolecular vibrational frequency reflects the curvature of the cage potential well. At the low-frequency region, different intermolecular vibrational modes coexist [5]. To avoid unfair comparison of the vibrational frequencies belonging to different modes in different liquids, the first moment of VDOS, $\langle\omega\rangle$, measuring the average characteristic frequency of intermolecular vibrations, were calculated for inorganic molten salts, ILs, and organic liquids in Ref. [6] (Eq. 3 and 4). As listed in Table 1, the calculated average characteristic frequencies (first moment) $\langle\omega\rangle$ agree with experimental data very well. We can see clearly that ILs show similar vibrational frequencies as molecular liquids DMSO and toluene, but much lower than molten NaCl. This result agrees well with the femtosecond Kerr effect spectroscopy measurements of an IL (1-methoxyethylpyridinium dicyanoamide) and its isoelectronic 1:1 solution of 1-methoxyethylbenzene and dicyanomethane, which were found to have similar vibrational modes and frequencies [7].

Under the harmonic approximation, the characteristic vibrational frequency directly relates to the vibrational force constant k via Eq. (5). The calculated force constants were listed in Table 1. Again, ILs have vibrational force constants k similar to molecular liquids, but much smaller than the molten salt, showing the unique organic nature of ILs.

Force and Intrinsic Electric Field

The organic nature of ILs not only controls the vibrational motion but also affects the strength of the intermolecular force. Figure 4a compares the distribution of the strength of the total intermolecular force ($\boldsymbol{F}_{tot} = \boldsymbol{F}_{elec} + \boldsymbol{F}_{vdw}$) experienced by each molecule in inorganic molten salts, ILs and molecular solvents [6]. Clearly, the strength of the intermolecular force in ILs is comparable to that in polar molecular liquid DMSO, slightly larger than weakly polar liquid toluene, but much smaller than molten NaCl by one order of magnitude.

As we have shown above, the charge delocalization and the excluded-volume effect are expected to significantly reduce the electrostatic

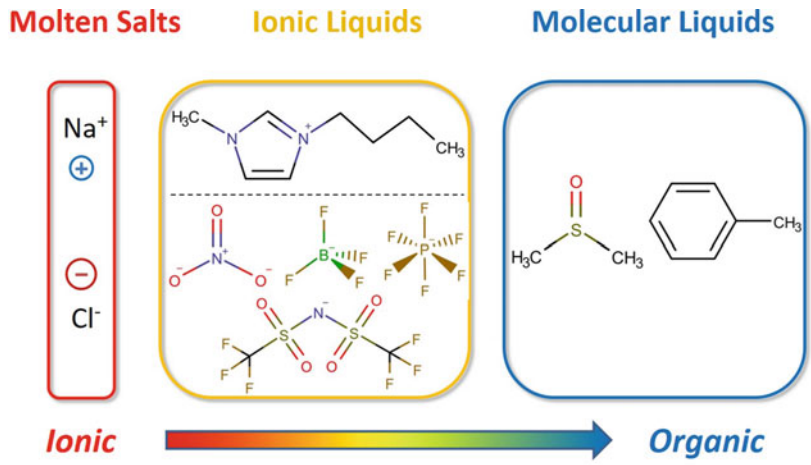

Dual Nature of Ionic Liquids: Ionic Versus Organic, Fig. 1 Molecular structures of typical molten salts, ionic liquids, and molecular liquids. From left to right: sodium chloride (NaCl), 1-butyl-3-methylimidazolium nitrate ([BMIm][NO_3]), 1-butyl-3-methylimidazolium tetrafluoroborate ([BMIm][BF_4]), 1-butyl-3-methylimidazolium hexafluorophosphate ([BMIm][PF_6]), 1-butyl-3-methylimidazolium bis(trifluoromethanesulfonyl)imide ([BMIm][NTf_2]), dimethyl sulfoxide (DMSO), and toluene, ordered from more ionic to more organic. (This plot is adapted from Fig. 1 of Ref. [6]. Reproduced with permission from Ref. [6]. Copyright 2016 Springer Nature)

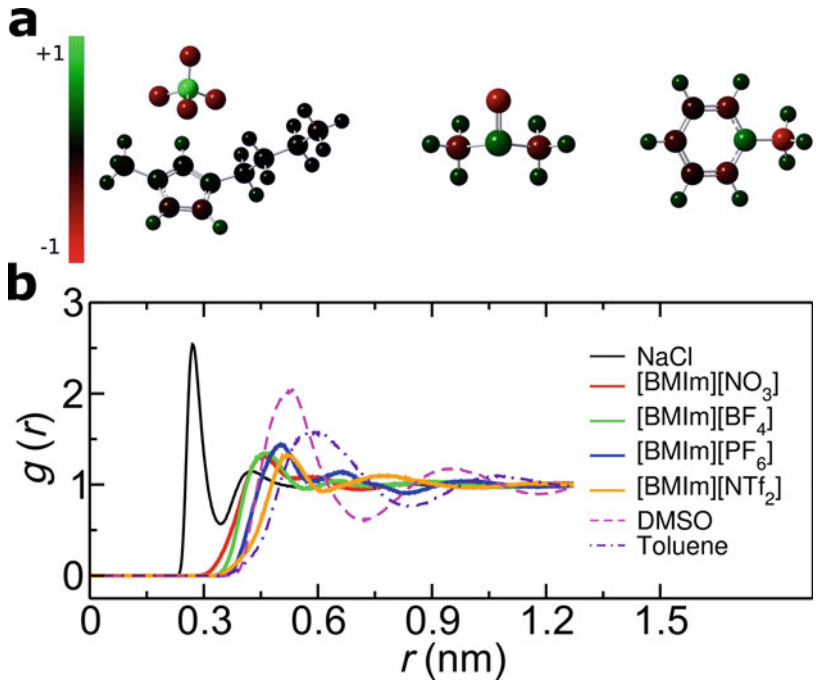

Dual Nature of Ionic Liquids: Ionic Versus Organic, Fig. 2 (**a**) From left to right, charge distributions of [BMIm][BF_4] ion pair, DMSO, and toluene molecules. The color bar indicates the amount of partial charge in the unit of the elementary charge *e*. (**b**) Center-of-mass radial distribution functions (COM-RDFs) of molten NaCl, [BMIm][NO_3], [BMIm][BF_4], [BMIm][PF_6], [BMIm][NTf_2], DMSO, and toluene. For ionic systems, cations and anions are treated identically. (Panels (a) and (b) are adapted from Figs. 2 and 3a of Ref. [6], respectively. Reproduced with permission from Ref. [6]. Copyright 2016 Springer Nature)

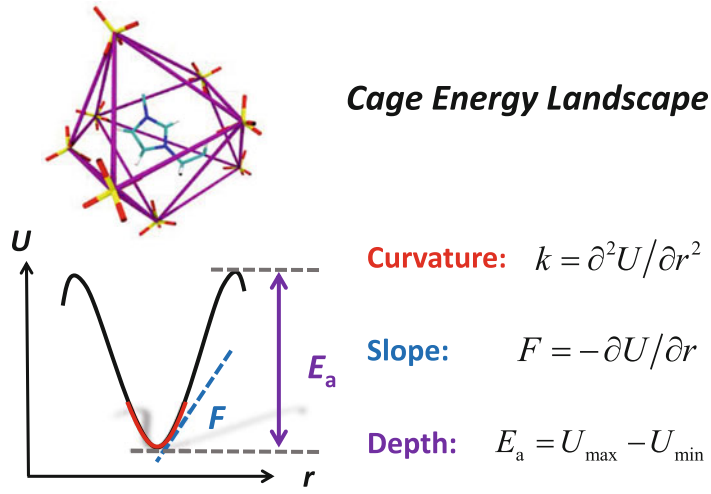

Dual Nature of Ionic Liquids: Ionic Versus Organic, Fig. 3 Cage structure ([BMIm][BF_4] as an example) and cage energy landscape. The cage energy landscape is a one-dimensional description of the average energy landscape experienced by each molecule, which is characterized by three parameters: curvature, slope, and depth, corresponding to the force constant, force, and activation energy, respectively. (This plot is adapted from Fig. 4 of Ref. [6]. Reproduced with permission from Ref. [6]. Copyright 2016 Springer Nature)

Dual Nature of Ionic Liquids: Ionic Versus Organic, Table 1 Average characteristic frequency (first moment) $\langle\omega\rangle$ of intermolecular vibrational mode and corresponding vibrational force constant *k*. The values in parentheses are experimental data. (This table is adapted from Table 2 of Ref. [6])

	$\langle\omega\rangle$/ cm^{-1}	k/ 10^{26} s^{-2}
NaCl	162 (–)	9.3
[BMIm][NO_3]	86(–)	2.6
[BMIm][BF_4]	82 (85)	2.4
[BMIm][PF_6]	76 (78)	2.0
[BMIm][NTf_2]	76 (77)	2.0
DMSO	77 (82)	2.1
Toluene	69 (66)	1.7

force in ILs. This is confirmed in Fig. 4b by showing the distribution of the electrostatic contribution (α, see inset of Fig. 4b for the definition) to the total intermolecular force. It can be seen that ILs and organic solvents commonly have a sharp peak around $\alpha = 0$, indicating strong VDW but rather weak electrostatic forces in these two classes of liquids. On the other hand, molten NaCl shows a much wider distribution of α than ILs and organic liquids, suggesting its strong ionic nature. This result is consistent with first principle calculations showing that the VDW interaction is negligible in a NaCl pair but plays an important role for the interactions between an IL pair [8].

The organic nature of ILs, giving rise to strong VDW but weak Coulomb interactions, similar to organic liquids, has been supported by a corresponding-states analysis of experimental surface tension data. As shown in Fig. 5a, Weiss has reported that the reduced surface tension γ_{red} of ILs follows a universal function $\gamma_{red} = \gamma_0 (1 - T/T_c)^{11/9}$ for simple molecular liquids, but deviates from that of inorganic molten salts, where T_c is the critical temperature and γ_0 is a constant [9].

Another direct experimental support of the organic nature of ILs comes from the measurement of the intrinsic electric fields in ILs and organic liquids. By using vibrational Stark effect spectroscopy, Zhang and coworkers successfully measured the nitrile stretching frequency $\nu C{\equiv}N$ of a probe molecule in ILs and organic liquids, which is found to be negatively proportional to the local electric field in the probed liquids [10]. As shown in Fig. 5b, the strengths of the electric fields in a group of ILs with different anions and different side chain lengths, except for [BMIm][Cl], all fall in the range of commonly used molecular liquids. Due to the small anion size, [BMIm]

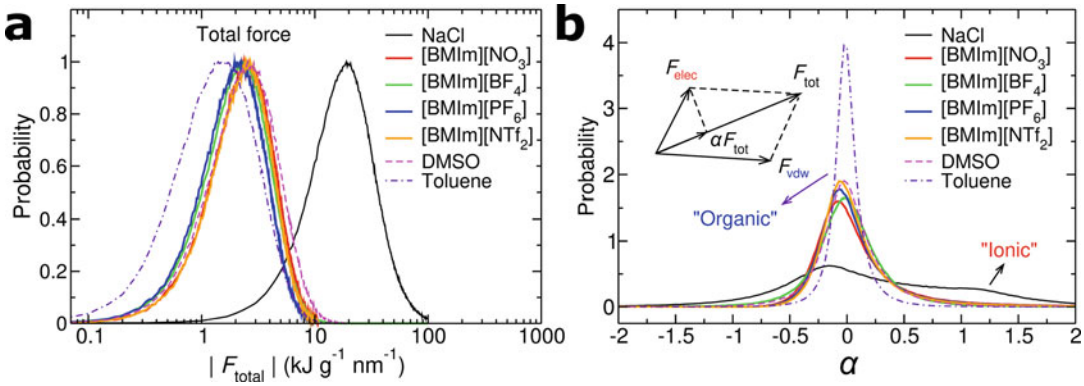

Dual Nature of Ionic Liquids: Ionic Versus Organic, Fig. 4 (**a**) Distribution of the strength of the total force experienced by each molecule in molten NaCl, [BMIm][NO_3], [BMIm] [BF_4], [BMIm][PF_6], [BMIm] [NTf_2], DMSO, and toluene. (**b**) Contribution of electrostatic interaction to intermolecular force. The contribution is described by a parameter $\alpha = \mathbf{F}_{\text{tot}} \cdot \mathbf{F}_{\text{elect}} / \mathbf{F}_{\text{tot}}^2$. The inset illustrates the decomposition of total force into electrostatic and VDW contributions. A peak at $\alpha = 0$ suggests a predominant contribution of VDW interaction to intermolecular force in ILs and organic solvents. The width of the distribution (normalized by area) characterizes the organic and ionic nature of forces in liquids: narrower means more organic and wider means more ionic. (This figure is adapted from Fig. 5 of Ref. [6]. Reproduced with permission from Ref. [6]. Copyright 2016 Springer Nature)

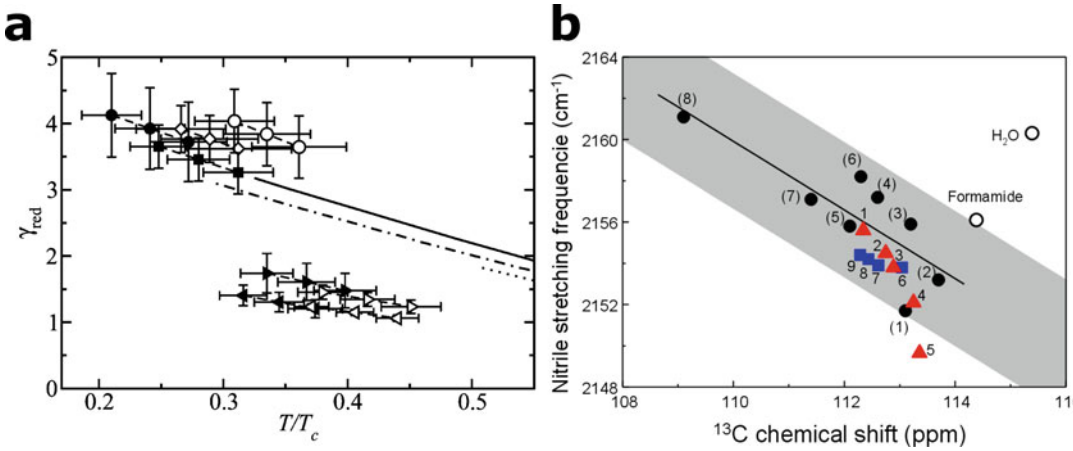

Dual Nature of Ionic Liquids: Ionic Versus Organic, Fig. 5 (**a**) Reduced surface tension $\left(\gamma_{\text{red}} \equiv c_0 M_r^{2/3} \gamma / \left(\rho_c^{2/3} T_c\right)\right)$ as a function of the reduced temperature T/T_c for the ionic liquids [EMIm][NTf_2] (filled circles), [BMIm][NTf_2] (filled squares), [HMIm] [NTf_2] (open diamonds), and [OMIm][NTf_2] (open circles), where γ is the surface tension, T_c is the critical temperature, ρ_c is the critical density, M_r is the molar mass, and c_0 is a constant. Lines represent data for typical molecular liquids, $CHClF_2$ (solid fine), methane (dotted fine), and ethane (dash dotted fine). Triangles denote data for inorganic molten salts, such as NaCl (triangles left) and KCl (triangles right). (The panel (a) is reproduced from Fig. 3 of Ref. [9]. Reproduced with permission from Ref. [9]. Copyright 2010 American Chemical Society). (**b**) Nitrile stretching frequencies νC≡N versus ^{13}C chemical shifts $\delta(^{13}\text{CN})$ in ILs and molecular solvents. Molecular liquids (filled black circle): (1) DMSO, (2) DMF, (3) acetone, (4) CD_2Cl_2, (5) THF, (6) $CDCl_3$, (7) toluene, (8) cyclohexane. [BMIm][X] ILs (filled red triangle): 1-[BMIm][NTf_2], 2-[BMIm][PF_6], 3-[BMIm][BF_4], 4-[BMIm][NO_3], 5-[BMIm][Cl]. [CnMIm][BF_4] ILs (filled blue square): 6-[EMIm][BF_4], 7-[HMIm][BF_4], 8-[OMIm][BF_4], and 9-[DMIm][BF_4]. The black fine shows the best linear fit for the νC≡N versus ^{13}C NMR data of molecular liquids excluding H-bonding liquids. (Panel (b) is adapted from Fig. 2A of Ref. [10]. Reproduced with permission from Ref. [10]. Copyright 2012 WILEYVCH Verlag GmbH & Co. KGaA, Weinheim)

[Cl] has an intrinsic electric field slightly larger than that of molecular liquids. This measurement, in quantitative agreement with molecular dynamics results [6, 10], strongly suggests the organic nature of ILs.

Cage Energy

The cage energy U_{cage} is defined as the average two-body interaction energy between the central molecule and the neighbors in the first coordination shell, characterizing the energy scale of the local intermolecular interactions in the liquids. A molecule has to overcome the cage energy to escape the cage and make a translational and/or rotational motion. Therefore, the cage energy is linked to the dynamic properties of a liquid. The calculated cage energy and its electrostatic and VDW contributions are listed in Table 2 [6]. It can be seen that ILs, similar to inorganic salts, commonly have much lower (negative) cage energies than molecular liquids. The low cage energy in the molten NaCl and ILs predominantly comes from the long-range Coulomb interactions, whereas the VDW force only has a minor contribution. On the other hand, the electrostatic contribution to the cage energy is very small and comparable to the VDW contribution for the strongly polar liquid DMSO, and even smaller than the VDW one for the weakly polar liquid toluene.

The long-range Coulomb interactions stabilizing the cage structure are responsible for the slow dynamics of ILs. This can be seen from the larger activation energy of ILs than organic liquids, which leads to a much larger viscosity of the former than the latter. The viscosity of molten NaCl is small, simply because it is measured at a very high temperature above the melting point.

Tune the Dual Nature of Ionic Liquids

The introduction of bulky organic ions effectively weakens the Coulomb interactions between ions, giving rise to the dual ionic and organic nature of ILs. Such a physical mechanism generally applies to ILs composed of organic ions. On the other hand, the dual nature of ILs can be tuned in a specific manner by chemical substitutions. For example, introduction of the ether [11–14] or hydroxyl groups [2, 15, 16] to the alkyl chain of cations can substantially change the structure and dynamics of ILs by forming additional hydrogen bonds between the functional groups and the ions, which is characteristic of the organic/molecular liquids.

Changing the length of the alkyl chain of the cation and/or anion is another way to tune the dual nature of ILs. As the length of the alkyl chain increases, ionic liquids form nanoscale aggregations of nonpolar alkyl chains separated by the continuous charge network [17–19]. A typical snapshot from coarse-graining molecular dynamics simulation [20] for the nanoscale aggregations is shown in Figure 7a. Such spatially heterogeneous structure, featuring a sharp prepeak in the structure factor [21], has been confirmed by the X-ray scattering experiments [22] (see Fig. 7b). Further increase of the length of the alkyl chain can lead to the formation of ionic liquid crystals of smectic type [4, 23–31] (see Fig. 7c for an example of $[C_{22}MIm][NO_3]$ ionic liquid crystal). The emergence of such unique structure features (nanoscale aggregations and smectic phase) as a consequence of the competition between the electrostatic and VDW interactions [4] reflects the dual nature of ILs.

Tuning the dual nature of ILs can have significant impact on the physicochemical properties of ILs. For example, it has been shown that the solubility of benzene in viologen bistriflimide increases linearly with the alkyl side-chain length [32]. The benzene molecules are favorably absorbed inside the nanoscale domains of the alkyl side chains due to their organic nature, which effectively fluidize the viologen salt and lead to the formation of a sponge-like liquid phase [32] (see Fig. 7d). Not only the static properties but also the dynamics are strongly affected by the dual nature of ILs. For example, it has been shown that the local friction experienced by a small tracer molecule is higher in the charge network than the nonpolar aggregation regions [33–36], well known as the dynamic heterogeneity [37]. Understanding the dual nature and its intrinsic relation to the physicochemical properties of

Dual Nature of Ionic Liquids: Ionic Versus Organic, Table 2 Cage energy U_{cage} with its electrostatic U_{cage}^{elec} and VDW component U_{cage}^{vdw} in kJ/mol from simulations, experimental viscosity η in mPas, experimental activation energy for diffusion E_a in kJ/mol (averaged over cation and anion), and experimental melting temperature in K. The VDW interaction is further decomposed into the attractive and repulsive parts, respectively, as listed in the parentheses. The data were calculated or measured at around 1150 K for NaCl and 300 K for other liquids. (See Ref. [6] for the details. This table is adapted from Tables 1, 4 and S1 of Ref. [6])

	U_{cage}	U_{cage}^{elec}	U_{cage}^{vdw}	η	E_a	T_m
NaCl	−453.7	−464.5	10.8 (−1.6, 12.4)	0.891	34.0	1073.15
[BMIm][NO_3]	−217.4	−213.9	−3.5 (−11.4, 7.9)	165.3	–	309.2
[BMIm][BF_4]	−162.8	−159.3	−3.5 (−10.7, 7.2)	90.04	33.45	188.15
[BMIm][PF_6]	−238.4	−233.8	−4.6 (−13.5, 8.9)	228.8	38.35	283.15
[BMIm][NTf_2]	−226.4	−215.6	−10.8 (−23.8, 13.0)	45.7	28.15	270.15
DMSO	−7.2	−3.6	−3.6 (−7.6, 4.0)	1.97	19.0	291.65
Toluene	−4.5	−0.4	−4.1 (−7.2, 3.1)	0.56	10.6	178.15

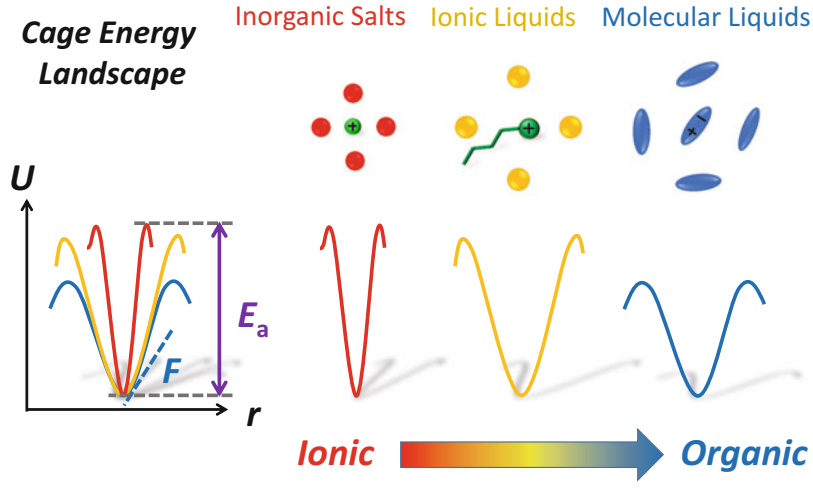

Dual Nature of Ionic Liquids: Ionic Versus Organic, Fig. 6 Schematic illustration of cage structures and cage energy landscapes in inorganic molten salts, ionic liquids, and molecular liquids. Inorganic molten salts have much steeper and deeper cage energy landscapes than molecular liquids. On one hand, the cage energy landscape of ionic liquids has similar slope and curvature to molecular liquids; on the other hand, its depth is comparable to molten salts. (This figure is adapted from Fig. 6 of Ref. [6]. Reproduced with permission from Ref. [6]. Copyright (2016) Springer Nature)

ILs is therefore crucial for designing new ILs with optimized performance.

Future Directions

Taken together, a microscopic physical mechanism of the dual nature of ILs emerges from the above discussions, in terms of the cage energy landscape (see Fig. 6). On one hand, the curvature-related properties of an IL, such as vibration, and slope-related ones, such as electric field, of the cage energy landscape show typical behaviors as polar organic liquids, which reflects the organic nature of ILs. On the other hand, the dynamic properties of an IL, linked to the height of the cage energy landscape, show unique behaviors, e.g., conductivity and slow mobility, different from organic liquids, characterizing the ionic nature of ILs.

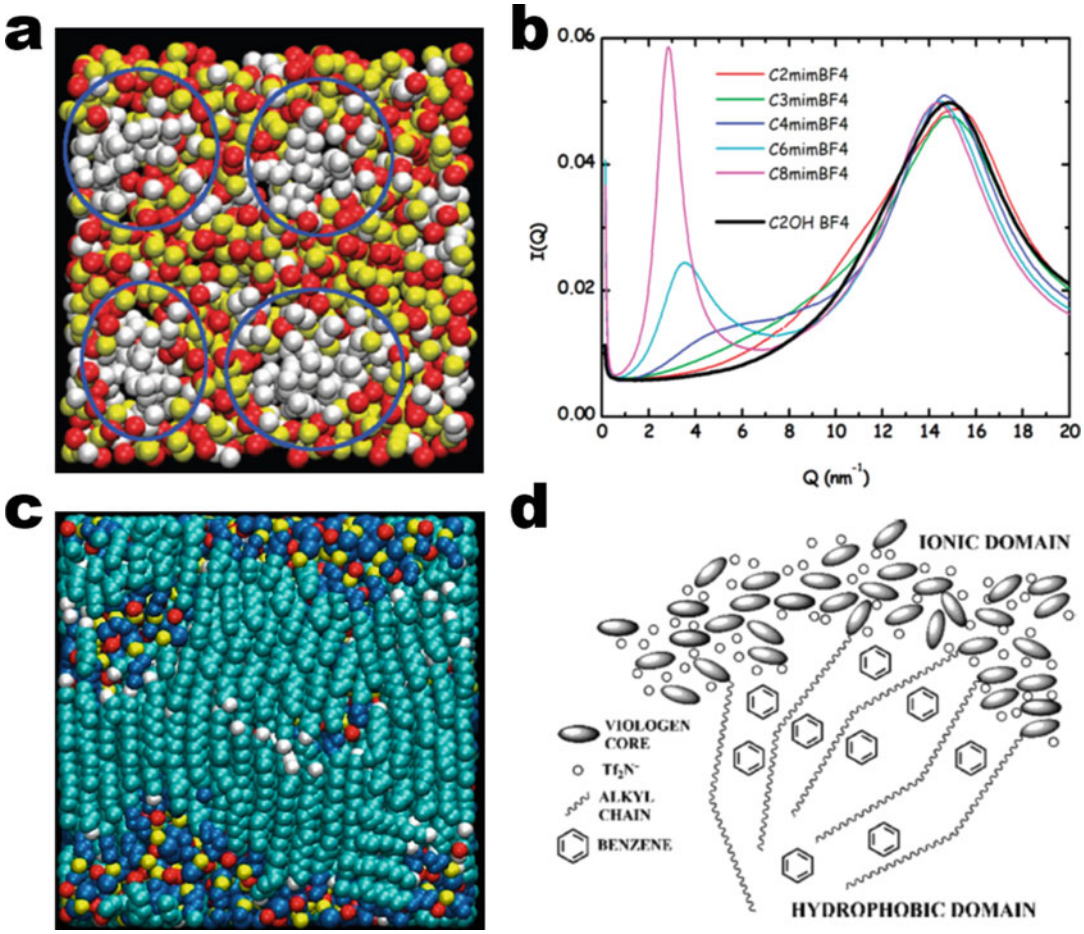

Dual Nature of Ionic Liquids: Ionic Versus Organic, Fig. 7 (**a**) A snapshot from coarse-graining molecular dynamics simulation showing the nanoscale aggregations of alkyl side chains (see blue ellipses) The white, yellow, red balls represent alkyl side chains, cationic head groups, and anions, respectively. (Reproduced with permission from Ref. [20]. Copyright (2007) American Chemical Society). (**b**) Structure factor of 1-alkyl-3-methylimidazolium tetrafluoroborate measured by X-ray scattering experiment at ambient condition [22]. The sharp prepeak signals the formation of nanoscale aggregations of alkyl side chains. (Reproduced with permission from Ref. [22]. Copyright (2012) American Chemical Society). (**c**) A snapshot from coarse-graining molecular dynamics simulation illustrating the structure of ionic liquid crystal. (Reproduced with permission from Ref. [4]. Copyright (2013) American Chemical Society). (**d**) Schematic illustration of the structure of benzene/viologen bistriflimide mixture. Benzene molecules preferentially stay in the nonpolar aggregation region of alkyl side chains. (Reproduced with permission from Ref. [32]. Copyright (2020) American Chemical Society)

The competition and balance between the organic and ionic nature determine the overall properties of an IL. For example, the ionic nature gives rise to nonflammability, non-volatility, good stability and conductivity of ILs, but also leads to slow dynamics, which greatly retards the application of ILs as electrolytes in energy-storage devices. How to design optimized ILs for a given application by tuning molecular structure, interactions, and consequently the balance between the dual nature of ILs still remains a major challenge in both academia and industry.

The mixing of IL with another (or more) component to make IL-IL mixtures [38], IL-molecular solvent mixtures [39], and solvate ILs [40, 41] provides additional degree of freedom, i.e., the composition of the mixture, to tune the balance of different nature and the underlying interactions of

different components and thus control the physicochemical properties of the system. Another interesting direction is to generate and explore the biological nature of ILs with tunable biocompatibility and bioactivity [40, 42]. Knowledges on the specific IL-biomolecule interactions are crucial for the exploration and design of bioactive ILs.

Cross-References

► Molecular Dynamics Simulation Method

References

1. Matthews RP, Welton T, Hunt PA (2014) Competitive pi interactions and hydrogen bonding within imidazolium ionic liquids. Phys Chem Chem Phys 16(7):3238
2. Deng L, Shi R, Wang Y, Ou-Yang ZC (2013) Hydrogen-bond rich ionic liquids with hydroxyl cationic tails. Chem Phys Lett 560:32
3. Strate A, Niemann T, Michalik D, Ludwig R (2017) When like charged ions attract in ionic liquids: Controlling the formation of cationic clusters by the interaction strength of the counterions. Angew Chem Int Ed 56(2):496
4. Ji Y, Shi R, Wang Y, Saielli G (2013) Effect of the chain length on the structure of ionic liquids: from spatial heterogeneity to ionic liquid crystals. J Phys Chem B 117(4):1104
5. Fumino K, Wulf A, Ludwig R (2008) The cation–anion interaction in ionic liquids probed by far-infrared spectroscopy. Angew Chem Int Ed 47(20):3830
6. Shi R, Wang Y (2016) Dual ionic and organic nature of ionic liquids. Sci Rep 6:19644
7. Shirota H, Castner EW (2005) Physical properties and intermolecular dynamics of an ionic liquid compared with its isoelectronic neutral binary solution. J Phys Chem A 109(42):9388
8. Zahn S, Uhlig F, Thar J, Spickermann C, Kirchner B (2008) Intermolecular forces in an ionic liquid ([Mmim][Cl]) versus those in a typical salt (NaCl). Angew Chem Int Ed 47(19):3639
9. Weiss VC (2010) Guggenheim's rule and the enthalpy of vaporization of simple and polar fluids, molten salts, and room temperature ionic liquids. J Phys Chem B 114(28):9183
10. Zhang S, Shi R, Ma X, Lu L, He Y, Zhang X, Wang Y, Deng Y (2012) Intrinsic electric fields in ionic liquids determined by vibrational stark effect spectroscopy and molecular dynamics simulation. Chem Eur J 18 (38):11904
11. Zhang S, Chen Z, Qi X, Deng Y (2012) Distinct influence of the anion and ether group on the polarity of ammonium and imidazolium ionic liquids. New J Chem 36(4):1043
12. Chen ZJ, Huo Y, Cao J, Xu L, Zhang S (2016) Physicochemical properties of ether-functionalized ionic liquids: understanding their irregular variations with the ether chain length. Ind Eng Chem Res 55 (44):11589
13. Deng J, Bai L, Zeng S, Zhang X, Nie Y, Deng L, Zhang S (2016) Ether-functionalized ionic liquid based composite membranes for carbon dioxide separation. RSC Adv 6(51):45184
14. Zhou Y, Xu X, Wang Z, Gong S, Chen H, Yu Z, Kiefer J (2020) The effect of introducing an ether group into an imidazolium-based ionic liquid in binary mixtures with DMSO. Phys Chem Chem Phys 22(27):15734
15. Zhang S, Qi X, Ma X, Lu L, Deng Y (2010) Hydroxyl ionic liquids: the differentiating effect of hydroxyl on polarity due to ionic hydrogen bonds between hydroxyl and anions. J Phys Chem B 114(11):3912
16. Wang L, Jin X, Li P, Zhang J, He H, Zhang S (2014) Hydroxyl-functionalized ionic liquid promoted CO_2 fixation according to electrostatic attraction and hydrogen bonding interaction. Ind Eng Chem Res 53 (20):8426
17. Wang Y, Voth GA (2005) Unique spatial heterogeneity in ionic liquids. J Am Chem Soc 127(35):12192
18. Canongia Lopes JN, Padua AA (2006) Nanostructural organization in ionic liquids. J Phys Chem B 110 (7):3330
19. Bhargava B, Balasubramanian S, Klein ML (2008) Modelling room temperature ionic liquids. Chem Commun 29:3339
20. Wang Y, Jiang W, Yan T, Voth GA (2007) Understanding ionic liquids through atomistic and coarse-grained molecular dynamics simulations. Acc Chem Res 40 (11):1193
21. Urahata SM, Ribeiro MC (2004) Structure of ionic liquids of 1-alkyl-3-methylimidazolium cations: A systematic computer simulation study. J Chem Phys 120(4):1855
22. Russina O, Triolo A, Gontrani L, Caminiti R (2012) Mesoscopic structural heterogeneities in room-temperature ionic liquids. J Phys Chem Lett 3(1):27
23. Binnemans K (2005) Ionic liquid crystals. Chem Rev 105(11):4148
24. Causin V, Saielli G (2009) Effect of asymmetric substitution on the mesomorphic behaviour of low-melting viologen salts of bis(trifluoromethanesulfonyl) amide. J Mater Chem 19(48):9153
25. Starkulla G, Klenk S, Butschies M, Tussetschlager S, Laschat S (2012) Towards room temperature ionic liquid crystals: linear versus bent imidazolium phenylpyrimidines. J Mater Chem 22(41):21987
26. Lava K, Evrard Y, Van Hecke K, Van Meervelt L, Binnemans K (2012) Quinolinium and isoquinolinium ionic liquid crystals. RSC Adv 2(21):8061
27. Saielli G, Bagno A, Wang Y (2015) Insights on the isotropic-to-smectic A transition in ionic liquid crystals from coarse-grained molecular dynamics

simulations: the role of microphase segregation. J Phys Chem B 119(9):3829
28. Saielli G, Wang Y (2016) Role of the electrostatic interactions in the stabilization of ionic liquid crystals: insights from coarse-grained MD simulations of an imidazolium model. J Phys Chem B 120(34):9152
29. Li S, Wang Y (2019) Percolation phase transition from ionic liquids to ionic liquid crystals. Sci Rep 9 (1):13169
30. Cao W, Wang Y (2019) Phase behaviors of ionic liquids heating from different crystal polymorphs toward the same smectic-A ionic liquid crystal by molecular dynamics simulation. Crystals 9(1):26
31. Cao W, Senthilkumar B, Causin V, Swamy VP, Wang Y, Saielli G (2020) Influence of the ion size on the stability of the smectic phase of ionic liquid crystals. Soft Matter 16(2):411
32. Li S, Safari N, Saielli G, Wang Y (2020) Liquid-liquid phase separation of viologen bistriflimide/benzene mixtures: role of the dual ionic and organic nature of ionic liquids. J Phys Chem B 124(36):7929
33. Araque JC, Hettige JJ, Margulis CJ (2015) Modern room temperature ionic liquids, a simple guide to understanding their structure and how it may relate to dynamics. J Phys Chem B 119(40):12727
34. Araque JC, Yadav SK, Shadeck M, Maroncelli M, Margulis CJ (2015) How is diffusion of neutral and charged tracers related to the structure and dynamics of a room-temperature ionic liquid? Large deviations from Stokes–Einstein behavior explained. J Phys Chem B 119(23):7015
35. Amith WD, Araque JC, Margulis CJ (2020) A pictorial view of viscosity in ionic liquids and the link to nanostructural heterogeneity. J Phys Chem Lett 11 (6):2062
36. Araque JC, Margulis CJ (2018) In an ionic liquid, high local friction is determined by the proximity to the charge network. J Chem Phys 149(14):144503
37. Hu Z, Margulis CJ (2006) Heterogeneity in a room-temperature ionic liquid: Persistent local environments and the red-edge effect. Proc Natl Acad Sci 103(4):831
38. Lian C, Liu K, Van Aken KL, Gogotsi Y, Wesolowski DJ, Liu H, Jiang D, Wu J (2016) Enhancing the capacitive performance of electric double-layer capacitors with ionic liquid mixtures. ACS Energy Lett 1(1):21
39. MacFarlane DR, Chong AL, Forsyth M, Kar M, Vijayaraghavan R, Somers A, Pringle JM (2018) New dimensions in salt–solvent mixtures: a 4th evolution of ionic liquids. Faraday Discuss 206:9
40. Angell CA, Ansari Y, Zhao Z (2012) Ionic liquids: past, present and future. Faraday Discuss 154:9
41. Watanabe M, Dokko K, Ueno K, Thomas ML (2018) From ionic liquids to solvate ionic liquids: challenges and opportunities for next generation battery electrolytes. Bull Chem Soc Jpn 91(11):1660
42. Hough WL, Smiglak M, Rodríguez H, Swatloski RP, Spear SK, Daly DT, Pernak J, Grisel JE, Carliss RD, Soutullo MD et al (2007) The third evolution of ionic liquids: active pharmaceutical ingredients. New J Chem 31(8):1429